Heliyon 11 (2025) e41601

Contents lists available at ScienceDirect

Heliyon

journal homepage: www.cell.com/heliyon

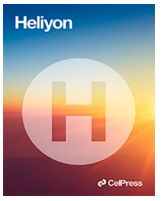

Research article

Comprehensive analysis reveals cholesterol metabolism-related signature for predicting prognosis and guiding individualized treatment of glioma

Dengfeng Lu [a,1], Fei Wang [a,1], Yayi Yang [a,b,1], Aojie Duan [a], Yubo Ren [a], Yun Feng [a,b], Haiying Teng [a], Zhouqing Chen [a,**], Xiaoou Sun [a,*], Zhong Wang [a,***]

[a] *Department of Neurosurgery & Brain and Nerve Research Laboratory, The First Affiliated Hospital of Soochow University, 188Shizi Street, Suzhou, 215006, Jiangsu Province, China*

[b] *Suzhou Medical College of Soochow University, Suzhou, Jiangsu Province, China*

ARTICLE INFO

Keywords:
Glioma
Cholesterol metabolism
Signature
Prognostic prediction
Immunoscape
Drug sensitivity

ABSTRACT

Objective: Gliomas are the most common intracranial tumors with the highest degree of malignancy. Disturbed cholesterol metabolism is one of the key features of many malignant tumors, including gliomas. This study aimed to investigate the significance of cholesterol metabolism-related genes in prognostic prediction and in guiding individualized treatment of patients with gliomas.

Methods: Transcriptional data and clinicopathological data were obtained from The Cancer Genome Atlas (TCGA) and Chinese Glioma Genome Atlas (CGGA) databases. Intraoperative glioma samples retained in our unit and the corresponding clinicopathological information were also collected with the patients' knowledge. Firstly, cholesterol metabolism-related gene signatures (CMRGS) were identified and constructed based on difference analysis, least absolute shrinkage and selection operator (LASSO) regression analysis, and univariate/multivariate COX analysis. Then, the role of CMRGS in predicting the prognosis of gliomas and distinguishing immune landscapes was evaluated by using nomograms, survival analysis, enrichment analysis, and immune-infiltration analysis. Finally, the drug sensitivity of gliomas in different risk groups was evaluated using the oncoPredict algorithm, and potentially sensitive chemotherapeutic and molecular-targeted drugs were identified.

Results: The prognostic CMRGS contained seven genes: APOE, SCD, CXCL16, FABP5, S100A11, TNFRSF12A, and ELOVL2. Patients were divided into high- and low-risk groups based on the median cholesterol metabolic index (CMI). There were significant differences in clinicopathological characteristics and overall survival between groups. COX analysis suggested that CMRGS was an independent risk factor for glioma prognosis and had a better predictive performance than several classical indicators. In addition, GSEA, immune infiltration analysis showed that CMRGS could differentiate the immune landscapes of patients in groups. The reliability of CMRGS was

* Corresponding author.
** Corresponding author.
*** Corresponding author.
E-mail addresses: 20227832023@stu.suda.edu.cn (D. Lu), wangfeiNeu@163.com (F. Wang), yy_yang_cn@163.com (Y. Yang), d362922899@163.com (A. Duan), yubo_ren0816@163.com (Y. Ren), Fengyun_0227@163.com (Y. Feng), 814382250@qq.com (H. Teng), zqchen6@163.com (Z. Chen), sunxo76@163.com (X. Sun), wangzhong761@163.com (Z. Wang).
[1] These authors contributed equally to this work.

https://doi.org/10.1016/j.heliyon.2024.e41601
Received 15 August 2024; Received in revised form 24 November 2024; Accepted 30 December 2024
Available online 2 January 2025

validated in the CGGA cohort and our Gusu cohort. Finally, 14 drugs sensitive to high-risk patients and 16 drugs sensitive to low-risk patients were identified.
Conclusion: The CMRGS reliably predicts glioma prognosis in multiple cohorts and may be useful in guiding individualized treatment.

1. Introduction

As the most common malignant tumor of the central nervous system (CNS), glioma is a global health threat with high morbidity and mortality. Gliomas usually originate from glial cells or precursor cells and develop into astrocytomas, oligodendrogliomas, glioblastomas (GBMs), etc. [1,2]. According to the fifth edition of the WHO Classification of Tumors of the Central Nervous System (WHO CNS5), gliomas are classified into WHO Grade 1–4; the higher the grade, the worse the prognosis. Generally, WHO Grades 1–2 are referred to as low-grade glioma (LGG), while WHO Grades 3–4 are termed high-grade glioma (HGG) [2]. Gliomas of WHO Grade 4 are the most malignant, with a median survival of fewer than two years, of which GBM accounts for the majority [3]. Treatment options for malignant tumors are usually one or a combination of surgical resection, radiotherapy, chemotherapy, immunotherapy and molecularly targeted therapy [4]. Advances in the above therapies have extended survival in glioma patients, but this is still far from satisfactory, especially for GBM patients [5,6]. There is an urgent need to identify new glioma markers to assess patients' prognosis and guide the direction of immunotherapy.

As an essential component of cell membranes and an important raw material for synthesizing steroid hormones, cholesterol is indispensable in regulating eukaryotic life processes such as cell membrane fluidity, membrane transport, and signal transduction [7,8]. The homeostatic balance of cholesterol in vivo is tightly regulated to maintain physiological functions [9]. Sources of cholesterol include endogenous synthesis and exogenous uptake. The related genes are transcriptionally regulated by sterol regulatory element-binding protein 2 (SREBP2), a transcription factor upregulating the expression of 3-hydroxy-3-methylglutaryl-coenzyme A reductase (HMGCR), a rate-limiting enzyme for cholesterol synthesis, and low-density lipoprotein (LDL) receptors associated with cholesterol uptake, thereby facilitating cholesterol biosynthesis and exogenous uptake [10–13]. The excretion of cholesterol includes producing cholesterol esters by Acyl coenzyme A-cholesterol acyltransferase (ACAT1) to be stored in lipid droplets, generating hydroxycholesterol by cholesterol hydroxylase, forming epoxycholesterol by cyclooxygenase [14,15]. In addition, cholesterol is transported by ATP-binding cassette transporter A1 (ABCA1) to apolipoprotein A-I (ApoA-I) to generate mature high-density lipoprotein (HDL), which is transported to the liver and converted to bile acids. In steroidogenic organs, cholesterol is taken as raw material to produce steroid hormones [11,13].

Altered cholesterol metabolism is a hallmark of many malignancies, including gliomas [16]. Abnormal cholesterol metabolism in tumor cells is mainly manifested by increased synthesis and uptake of cholesterol, and accumulation of large amounts of metabolites, leading to proliferation, invasion, metastasis, and enhanced adaptation to the tumor microenvironment, which promotes tumorigenesis and progression [17,18]. Series of evidence suggests that cholesterol metabolism is involved in maintaining the malignant progression of gliomas. GBM cells rely on external cholesterol to survive and accumulate lipid droplets to meet their rapid growth requirements [16]. HMGCR expression was upregulated in GBM cells, and LDL receptor expression was also higher than that of adjacent brain tissue, indicating enhanced cholesterol synthesis and uptake [19,20]. Thus, increased cholesterol synthesis is thought to promote glioblastoma growth [21,22]. Interestingly, macrophages are thought to be essential "cholesterol factories", providing cholesterol to promote GBM growth and induce $CD8^+$ T cell depletion [23]. In addition, modulation of cholesterol metabolism can promote an enhanced immune phenotype by triggering immunogenic cell death (ICD) and increasing cytotoxic T lymphocyte (CTL) infiltration in glioma [24]. In summary, targeting cholesterol metabolism may exert antitumor effects by inhibiting glioma cell growth and enhancing immunity [4,16].

The development of metabolism-related biomarkers can help in assessing the diagnosis and prognosis of a wide range of diseases [25]. Cholesterol metabolism-related biomarkers have been initially explored for clinical applications in a variety of tumors. The expression of squalene monooxygenase (SQLE), one of the key enzymes for cholesterol biosynthesis, is highly correlated with lethal prostate cancer, which has been validated in several cohorts [26]. Tang et al. showed that different cholesterol metabolism patterns were demonstrated to serve as predictive of prognosis and response to immunotherapy for gastric cancer biomarkers [27]. In addition, genetic signatures associated with dysregulation of cholesterol homeostasis have been suggested to be used as biomarkers for the diagnosis of a variety of cancers, including bladder and breast cancers [28]. This study focused on cholesterol metabolism-related genes through a series of bioinformatics approaches to explore their significance in predicting prognosis and guiding individualized treatment in glioma patients.

2. Methods

2.1. Acquisition of transcriptomic data and glioma sample collection

The transcriptomic data of glioma samples and the corresponding clinicopathologic data were obtained from The Cancer Genome Atlas (TCGA) (http://cancergenome.nih.gov/, used as the training set) and Chinese Glioma Genome Atlas (CGGA) database (http://www.cgga.org.cn/, used as the validation set), while the transcriptomic data of the control group (normal people) were obtained from Genotype-Tissue Expression Project (GTEx, https://www.gtexportal.org/home/index.html). Tissue specimens and clinicopathological

data, including age, gender, WHO grade, IDH mutation status, and MGMT promoter methylation status, were collected from eight glioma patients who underwent surgical treatment at the First Affiliated Hospital of Soochow University (hereinafter referred to as the Gusu cohort) between September 2022 and November 2023 in this study. All patients were treated for the first time with surgery and had not received any previous treatment. Each patient underwent complete microsurgical resection and was diagnosed with a glioma through a combined analysis performed by two skilled pathologists. The enrolled glioma patients consisted of two WHO grade 2, one WHO grade 3, and five GBM. In addition, 2 patients with traumatic brain injury provided normal brain tissue. All patients gave informed consent and signed. The entire study process was approved by the First Affiliated Hospital of Soochow University Ethics Committee on December 26, 2023 (Approval No. 524).

2.2. Identification of cholesterol metabolism-related genes

Cholesterol metabolism-related genes were obtained from the Molecular Signatures Database (https://www.gsea-msigdb.org/gsea/msigdb/index.jsp). Differential analysis of standardized FPKM data was performed based on the R package “limma”. Then, uni/multivariate COX regression analysis was performed by combining expression data and survival data using the R package “survival”. The machine learning algorithm least absolute shrinkage and selection operator (LASSO) regression was performed based on the R package “glmnet” due to its excellent feature in selection ability, interpretability, resistance to overfitting, and high computational efficiency [29]. All heatmaps in this study were calculated by z-score and plotted based on the R package "ComplexHeatmap". The forest plot is visualized using the R package "survminer".

2.3. Construction of risk model

The risk score here is referred to cholesterol metabolism index (CMI). The following formula was used to calculate the CMI for each patient, as previously reported:

$$CMI = \sum_{i=1}^{n} (\mathrm{iCoef}^{*}\mathrm{iExp})$$

Coef was calculated from the expression matrix and survival data by multivariate COX regression analysis, and Exp represents the expression value of the corresponding modeling gene. Patients were divided into high- and low-risk groups by the median CMI. The "survival" was used to plot the Kaplan-Meier (KM) curve to evaluate the survival difference between the two groups, and the "timeROC" R package was used to plot the ROC curve to evaluate the predictive performance of the model.

2.4. Construction of prognostic nomogram

Risk groups were combined with a series of clinicopathological characteristics, such as gender, age, race, grade, IDH mutation, MGMT promoter methylation status, etc., to construct a prognostic nomogram using the R package "rms", to predict the overall survival rate of glioma patients.

2.5. Functional enrichment analysis

Gene Set Enrichment Analysis (GSEA) is used to determine whether predefined sets of genes, rather than individual genes, differ significantly between two biological states. By revealing specific pathways associated with disease progression, for example, cell proliferation, immune response, or metabolism-related pathways in glioma progression, GSEA can help researchers more fully understand the role of entire biological pathways. In this study, functional enrichment analysis was performed by GSEA and R software using GO pathway analysis.

2.6. Characterization of immune landscape

Immune checkpoint expression, immune cell, and immune function scores were assessed between risk groups. In addition, ESTIMATEScore, ImmuneScore, and StromalScore were also compared between the two groups via the R package “estimate” to identify the prediction of CMRGS in the tumor microenvironment.

2.7. CGGA validation of CMRGS

Data from the CGGA cohort was used as external validation. As previously described, patients were divided into two groups based on median CMI, and further survival analysis and ROC analysis were performed based on the R package to assess the applicability of the CMRGS.

2.8. Validation of the Gusu Cohort

Samples of gliomas undergoing surgical treatment in our hospital (September 2022–November 2023) were collected and sent for

Bulk RNA sequence to calculate the CMI between different WHO grades based on the expression of CMRGs, to further assess the applicability of CMRGS.

2.9. Immunohistochemical staining

Paraffin-embedded glioma tissue slices were dewaxed and dehydrated for antigen repair and blocking to prevent nonspecific binding, as described previously [30]. This was followed by overnight incubation with diluted specific primary antibodies (10237-1-AP). Then after incubation with an anti-biotin-biotin horseradish peroxidase complex, HRP activity was detected under a light microscope with 3,3′-diaminobenzidine solution.

2.10. Targeted drug screening and characterization

Drug identification and sensitivity analyses were performed based on the "pharmacoGx" package and the "OncoPredict" package as described previously [31]. PharmacoDB 2.0 (https://pharmacodb.ca/) was used to visualize the IC50 of selected drug experiments between different tissues [32].

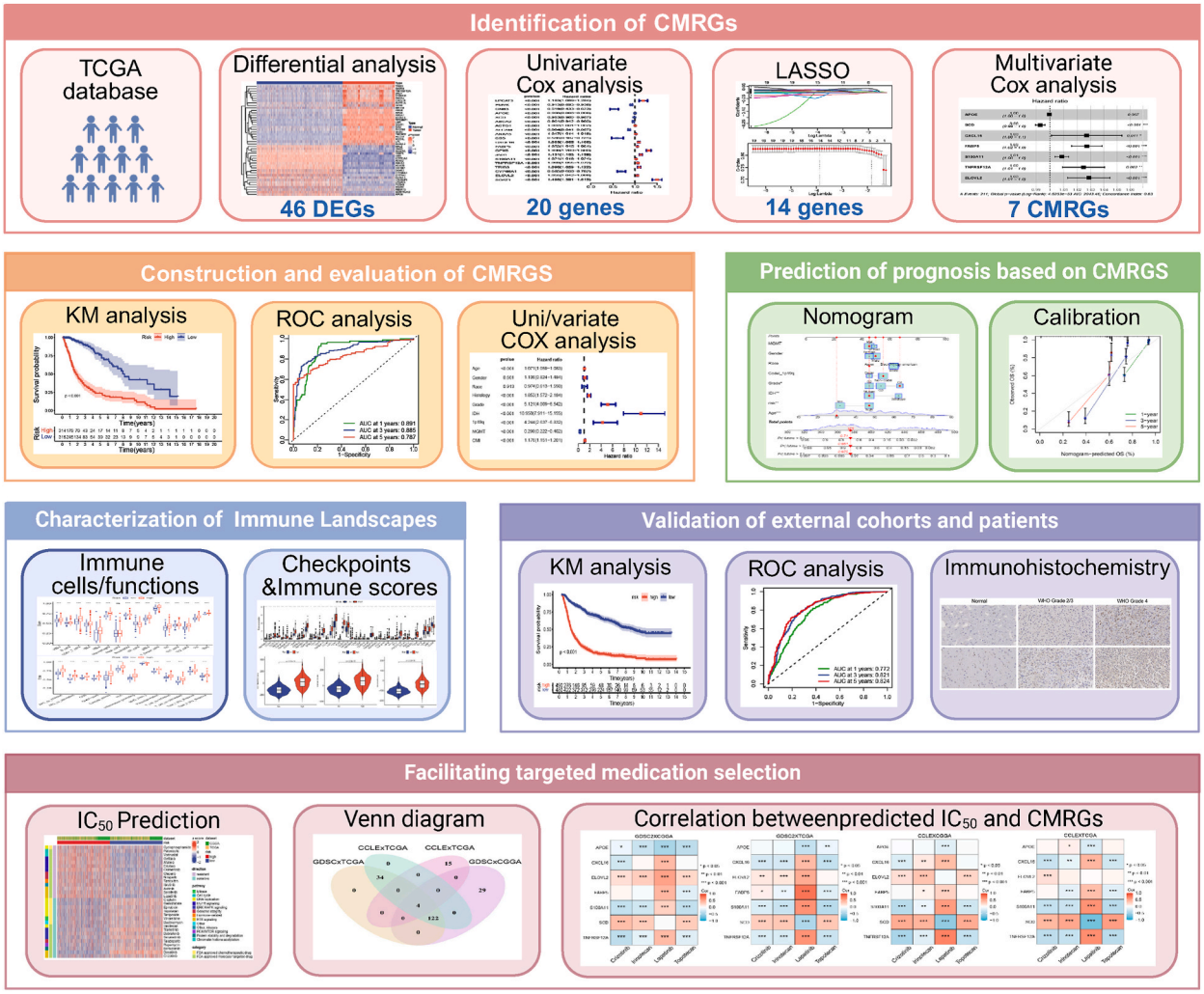

Fig. 1. Flowchart of this study.

2.11. Statistical analysis

RNA-seq transcriptome data were preprocessed using the Perl programming language (version 5.32.0). R software (version 4.2.1) was used for all statistical analyses and graphical visualization. Student's t-test, one-way ANOVA, and chi-square test were used to compare differences between risk groups. Kaplan-Meier (K-M) survival analysis and log-rank test were used to describe the survival distribution. p-value ≤ 0.05 was considered statistically significant.

3. Results

3.1. Identification of prognostic Cholesterol-Metabolism related differentially expressed genes in glioma

The flowchart of this study is shown in Fig. 1. Cholesterol metabolism-related genes (CMRGs) were obtained from the Molecular Signatures Database (https://www.gsea-msigdb.org/gsea/msigdb/index.jsp) [33–35]. First, 46 differentially expressed genes (DEGs) between the normal and glioma groups were identified by differential analysis (Fig. 2A). These DEGs were next characterized using

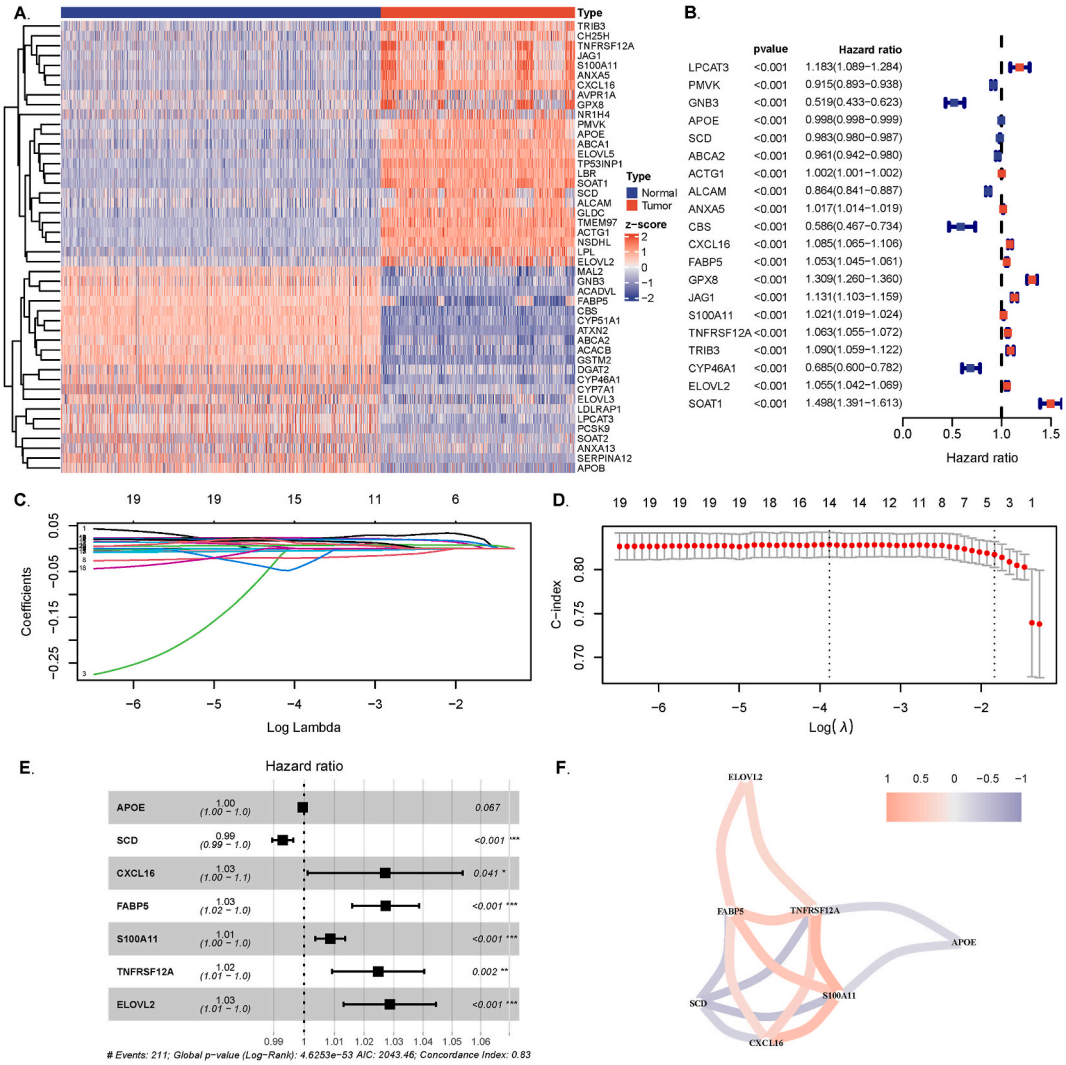

Fig. 2. Identification of prognostic Cholesterol-Metabolism-related genes from TCGA cohort. (A) Heatmap of 46 DEGs in normal and glioma groups. The redder, the higher the gene expression; the bluer, the lower the gene expression. (B) Forest plot of 20 Cholesterol-Metabolism-related genes performed by univariate Cox regression analysis. (C) LASSO coefficient profiles of Cholesterol-Metabolism-related genes. (D) Partial likelihood deviance of different numbers of variables revealed by the LASSO regression model (The log(λ) sequence plot of Cholesterol-Metabolism-related genes using LASSO regression). (E) Forest plot of 7 Cholesterol-Metabolism-related genes by multi-Cox regression. (F) Correlation between Cholesterol-Metabolism-related genes. DEG, differentially expressed gene; TCGA, The Cancer Genome Atlas; LASSO, least absolute shrinkage and selection operator.

gene ontology (GO) enrichment analysis and Kyoto Encyclopedia of Genes and Genomes (KEGG) pathway analysis (Figs. S1A and B). Most DEGs were found to be enriched in the pathways of cholesterol metabolism and homeostasis, steroid biosynthesis, fatty acid synthesis, and lipoprotein particles. Twenty genes were then identified by univariate Cox regression analysis based on transcriptomic data and clinical information from the TCGA database (Fig. 2B). Immediately following the incorporation of these genes in the LASSO regression to further refine the variables, 14 genes were identified (Fig. 2C and D). Finally, we identified 7 genes using multivariate Cox regression analysis: APOE, SCD, CXCL16, FABP5, S100A11, TNFRSF12A, and ELOVL2 (Fig. 2E). Thus, the identification of prognostic CMRGs was completed. Among them, CXCL16, FABP5, S100A11, TNFRSF12A, and ELOVL2 were prognostic risk factors for patients with hazard ratios (HRs) > 1, whereas APOE and SCD were protective factors with HRs <1. In addition, we identified the correlations among these CMRGs using Pearson correlation analysis. Fig. 2F shows the genes with correlation coefficients >0.2, with positive correlations in red and negative correlations in blue.

3.2. Construction of prognostic Cholesterol-Metabolism-related gene signature

The risk score was termed the Cholesterol-Metabolism Index (CMI), which was calculated as follows:

CMI = (−0.0005 * APOE exp) + (−0.0071 * SCD exp) + (0.0268 * CXCL16 exp) + (0.0269 * FABP5 exp) + (0.0086 * S100A11 exp) + (0.0244 * TNFRSF12A exp) + (0.0283 * ELOVL2 exp).

3.3. Evaluation of CMI in TCGA

The samples in the TCGA dataset were categorized into high- and low-risk groups based on median CMI, and a series of tests were performed to assess model performance. KM analysis showed that the survival probability was significantly higher in the low-risk group than in the high-risk group (Fig. 3A). As shown in the heatmap (Fig. 3B), the seven identified DEGs were differentially expressed in groups. ELOVL2, CXCL16, FABP5, S100A11, and TNFRSF12A were highly expressed in the high-risk group compared with the low-risk group, while APOE and SCD were expressed at lower levels. The TCGA cohort was divided into two groups based on the expression level of each modeled gene, and there was a significant difference in survival probability between these two groups (see Fig. S2). Specifically, those with high expression of APOE or SCD have higher survival probabilities, while the opposite was true for the other DEGs, which is consistent with the above findings. Besides, patients in the high-risk group had shorter survival times than those in the low-risk group. Specifically, the median survival times of patients in the high- and low-risk groups in the TCGA cohort were significantly different at 14.5 and 20.4 months, respectively. In addition, we performed principal component analysis (PCA) and t-distributed stochastic neighbor embedding analysis (t-SNE) on the samples in the TCGA cohort. The results showed significant differences in distribution between groups (Fig. 2C and S3A). Time-dependent receiver operating characteristic (ROC) curves were used

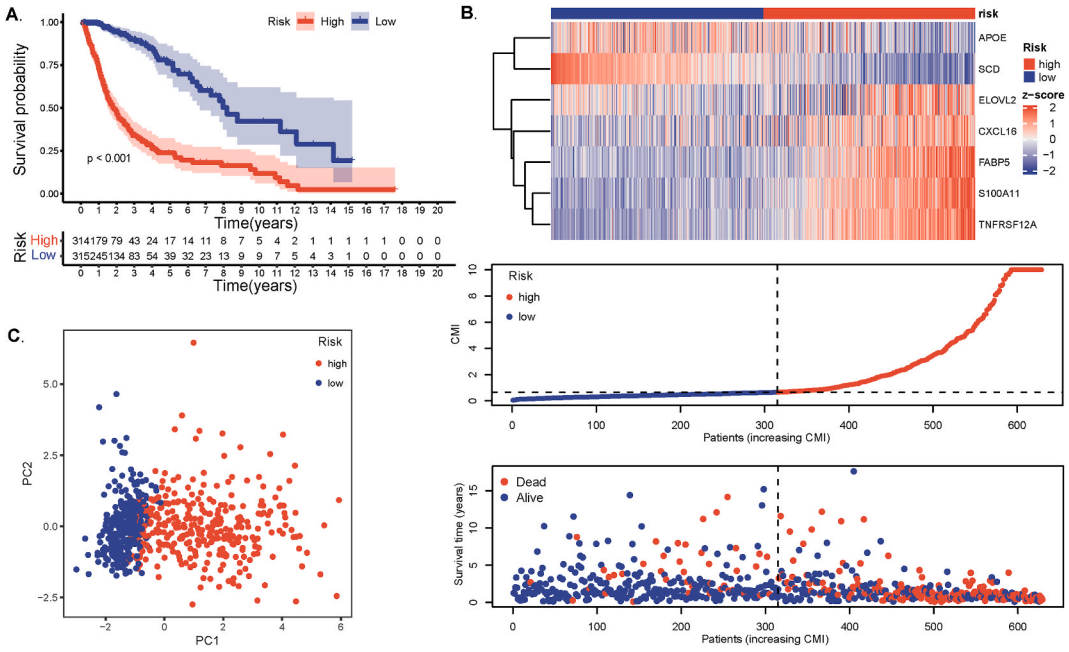

Fig. 3. Validation of CMRGS in TCGA cohort. (A) Overall survival of high- and low-risk groups according to CMI in glioma patients from TCGA. (B) Heatmap of expression of the seven modeling genes in high- and low-risk groups (upper), distribution and median value of CMI (middle), and the distribution of survival status and CMI (below). The redder, the higher the gene expression; the bluer, the lower the gene expression. (C) PCA analysis of CMRGS. CMRGS, Cholesterol-Metabolism-related genes signature; CMI, Cholesterol-Metabolism index; DEG, differentially expressed gene; PCA, principal component analysis.

to assess the effectiveness of CMI in predicting the prognosis of glioma patients. As shown in Fig. S3B, the AUCs for 1-, 3-, and 5-year overall survival (OS) in the TCGA dataset were 0.891, 0.885, and 0.787, respectively. Together, these results suggest that CMI can effectively predict the prognosis of glioma patients.

3.4. Independent prognostic value of CMRGS

A heatmap (Fig. 4A) containing CMRGS transcriptomic data and clinical features (MGMT promoter status, 1p19q co-deletion status, IDH mutation status, WHO grade, histology, race, gender, and age) showed that the expression of ELOVL2, CXCL16, FABP5, S100A11, and TNFRSF12A was positively correlated with CMI, while APOE and SCD negatively correlated. Patients in the high-risk group tended to have higher age, more histologic types of glioblastoma, higher WHO grade, more wild-type IDH, more non-co-deletion of 1p19q, and an unmethylated MGMT promoter. The differences of these clinical features in CMI are also shown in Supplementary Figs. S4–S6. The distribution of intergroup differences in the above characteristics is consistent with our current understanding of glioma. Multiple ROC analysis (Fig. 4B) showed that the predictive performance of CMI (AUC = 0.889) was superior to those of many classical indicators, including histology (AUC = 0.695), WHO grade (AUC = 0.804), IDH mutation status (AUC = 0.861), 1p19q co-deletion status (AUC = 0.639), and MGMT promoter status (AUC = 0.311). Univariate and multivariate Cox analysis of clinical and pathologic characteristics of glioma patients showed that CMI itself was an independent risk factor for glioma prognosis (Fig. 4C and D).

3.5. Establishment of a nomogram based on independent prognostic factors for OS and validation of its predictive accuracy

The excellent predictive performance of CMRGS makes us confident in expanding its clinical applicability. By incorporating risk grouping, age, gender, race, WHO grade, IDH mutation status, MGMT promoter status, and 1p19q co-deletion status, we built a comprehensive nomogram to predict 1-, 3-, and 5-year survival probabilities for glioma patients (Fig. 5A). The calibration curves showed good concordance between the predicted OS and the actual OS at 1, 3, and 5 years, demonstrating the predictive accuracy of the nomogram (Fig. 5B).

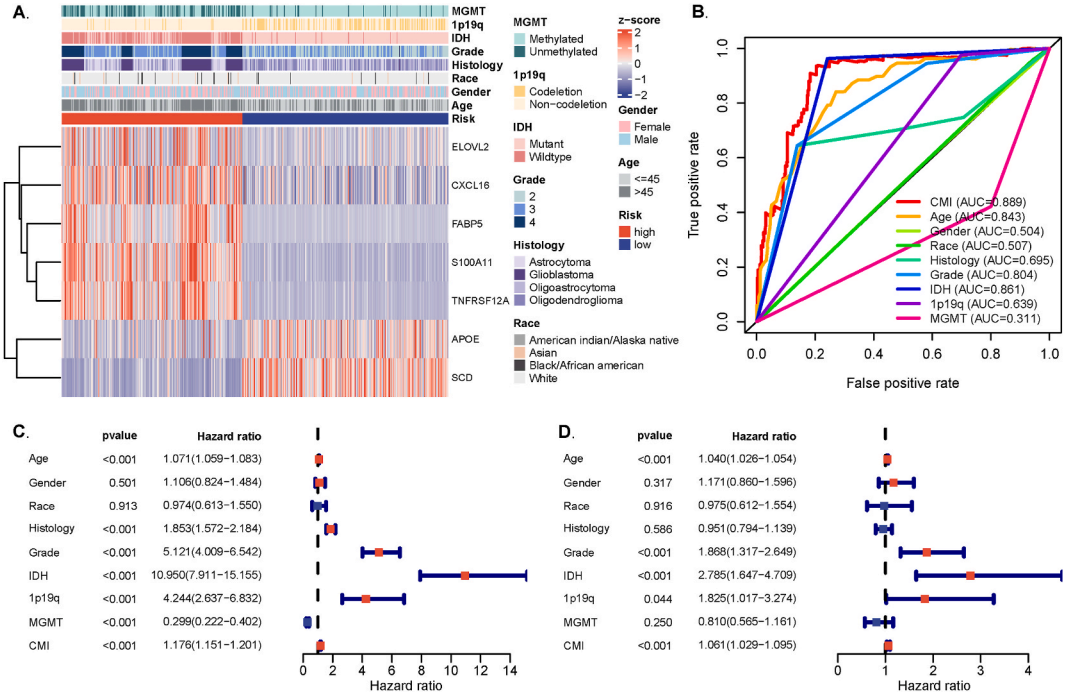

Fig. 4. Correlation between CMI and clinicopathological characteristics in TCGA dataset. (A) Heatmap of correlation between risk groups, age, gender, race, histology, grade, IDH mutation status, 1p19q mutation status, MGMT promoter status, and expression of Cholesterol-Metabolism-related genes. The redder, the higher the gene expression; the bluer, the lower the gene expression. (B) ROC curves of CMI and clinicopathological characteristics. (C and D) Univariate and multivariate Cox regression analysis of the combination of CMI and clinicopathological characteristics. CMI: Cholesterol-Metabolism index; IDH, isocitrate dehydrogenase; MGMT, O6-methylguanine-DNA methyltransferase; ROC, receiver operating characteristic.

3.6. Functional enrichment analysis

To explore the potential biological functions of CMRGS, we performed gene set enrichment analysis (GSEA) based on GO analysis. The results showed that adaptive immune response, immune effector processes, regulation of lymphocyte activation, response to the bacterium, and T-cell activation were significantly enriched in the high-risk group (Fig. 5C). Processes such as glutamatergic synapse, interneuronal synapse, postsynaptic membrane, bilateral tonic-clonic seizure, and myoclonus were remarkably enriched in the low-risk group (Fig. 5D). These biological differences suggested different immune activation processes between the high- and low-risk groups, providing some clues for future in-depth studies targeting gliomas.

3.7. Correlation analysis between prognostic CMRGS and immune landscape of glioma

We first evaluated the potential correlation between CMRGS and immune checkpoints (IC) (Fig. 6A). The results showed that almost all IC genes except CD200 were significantly upregulated in the high-risk group, implying a potential positive response to IC inhibitor therapy. Next, the expression patterns of multiple immune cells were analyzed between risk groups (Fig. 6B). Among them, aDCs, B cells, $CD8^+$ T cells, DCs, iDCs, macrophages, neutrophils, pDCs, T helper cells, Tfh, Th1 cells, Th2 cells, TIL, and Treg had higher expression abundance in the high-risk group, whereas NK cells were more abundant in the low-risk group (Fig. 6B). Similarly, the 13 immune processes included for assessment, including APC co-inhibition, APC co-stimulation, CCR, checkpoint, cytolytic activity, HLA, inflammation-promoting, MHC class I, parainflammation, T-cell co-inhibition, T-cell co-stimulation, type I IFN response, and type II IFN response, were more active in the high-risk group (Fig. 6C). The above evidence strongly suggested more intense antitumor immune activation in the high-risk group. In addition, we further assessed the relationship between CMRGS and glioma immune microenvironment (Fig. 6D). The ESTIMATE score, immune score, and stromal score were higher in the high-risk group than in the low-risk group, further suggesting a more abundant immune cell infiltration and a stronger level of immune response in the high-risk

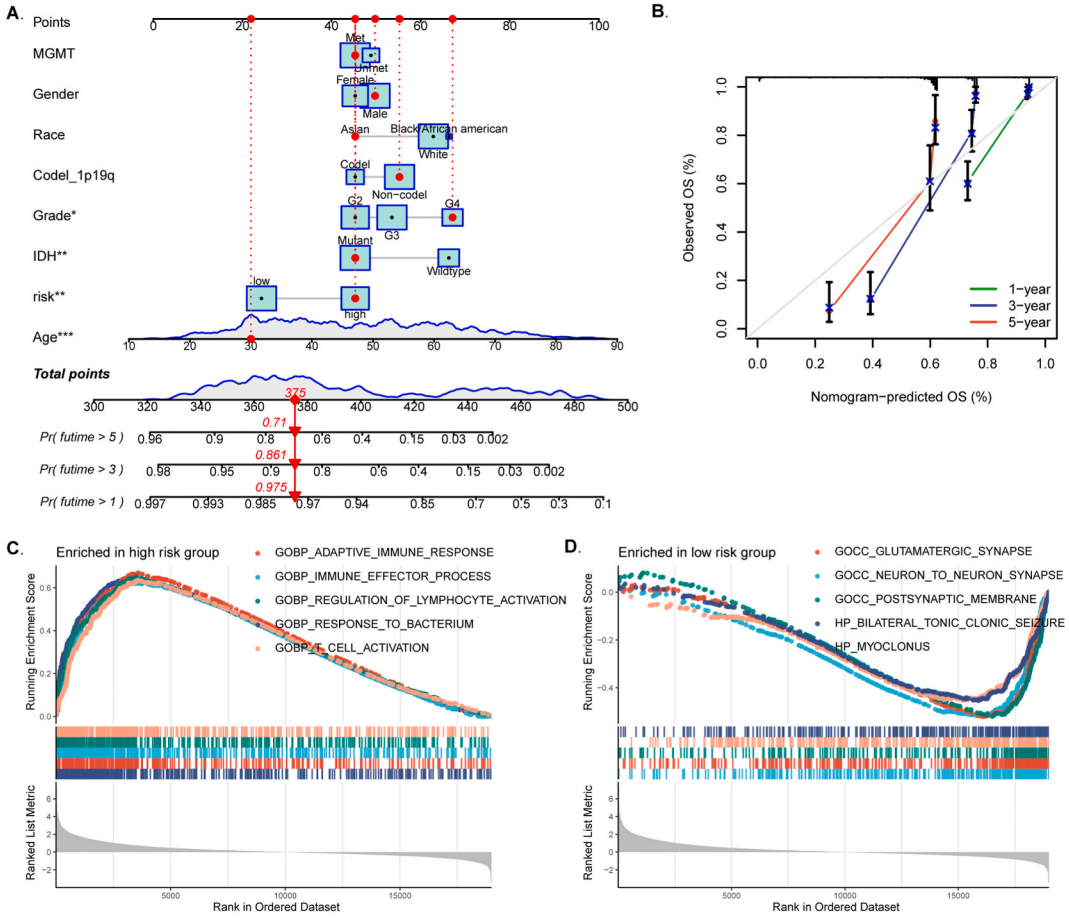

Fig. 5. Prediction of the survival of glioma patients by nomogram, and GSEA analysis between different risk groups in TCGA cohort. (A) Nomogram used for predicting glioma patients was constructed. (B) Calibration plots for predicting 1-, 3- and 5-year overall survival. (C and D) GSEA functional enrichment analysis base on GO pathway.GSEA, gene set enrichment analysis; TCGA, The Cancer Genome Atlas; GO, Gene Ontology. ***$p < 0.001$, **$p < 0.01$, *$p < 0.05$.

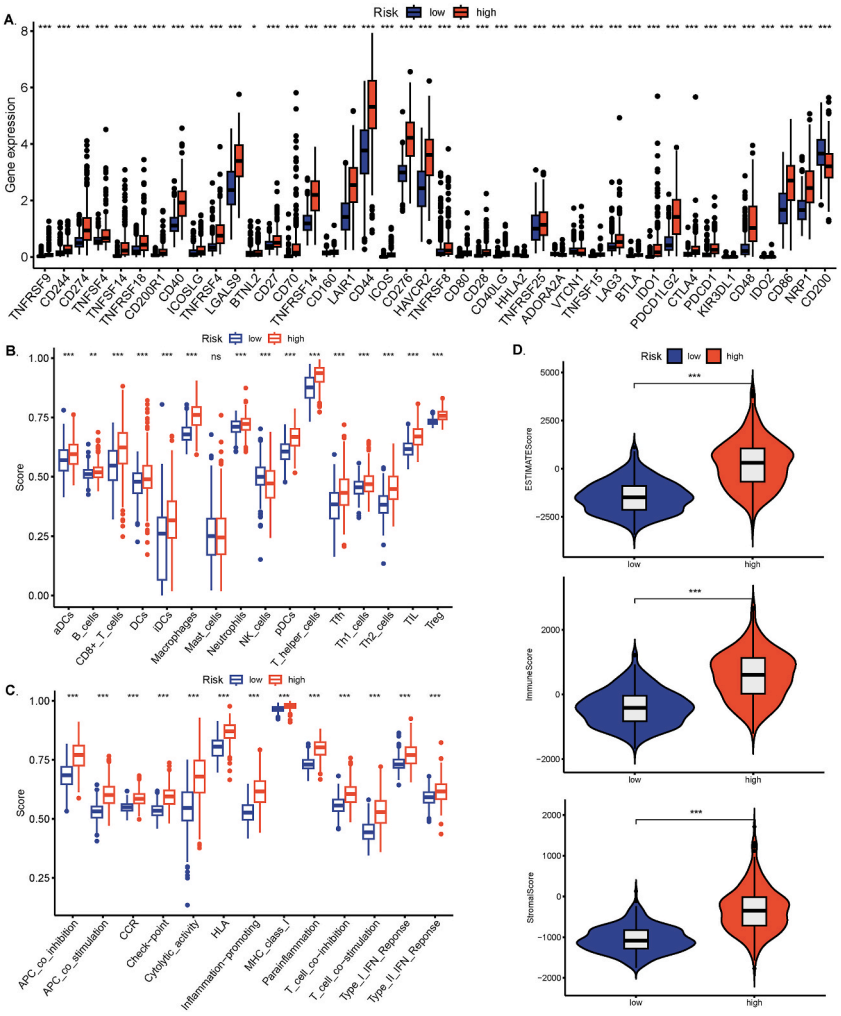

Fig. 6. Comparison of immune landscapes between high- and low-risk groups based on CMI. (A) Comparison of immune checkpoint expression levels in different groups. (B and C) Comparison of immune cells and immune function between groups.(D) Scores for glioma microenvironment in different groups.***$p < 0.001$, **$p < 0.01$, *$p < 0.05$.

group.

3.8. *Validation of the prognostic model in External Cohorts*

To confirm the universality of CMRGS in glioma patients, we performed an external validation based on the CGGA cohort. First, the glioma patients enrolled in CGGA were categorized into high-risk and low-risk groups based on their median risk score (Fig. 7B). It was found that the survival probability and survival time of the high-risk group were significantly lower than those of the low-risk group (Fig. 7A and B). Next, we performed ROC curve analysis to further assess the accuracy of CMRGS in predicting the prognosis of glioma patients in CGGA. the AUC at 1, 3, and 5 years were 0.772, 0.821, and 0.824, respectively (Fig. 7C). In addition, the expression patterns of the modeled genes in the CGGA cohort were consistent with those of the TCGA cohort (Fig. 7B). To further clarify the potential prognostic value of CMRGS in GBM, we utilized survival data from seven cohorts, including the Cancer Genome Atlas (TCGA, https://portal.gdc.cancer.gov), the Chinese Glioma Genome Atlas (CGGA, http://www.cgga.org.cn/index.jsp, CGGA693 and CGGA325), the Gene Expression Omnibus (GEO, https://www.ncbi.nlm.nih.gov/geo/, GSE121720 and GSE147352), the Glioma Longitudinal Analysis Series (GLASS, http://www.synapse.org/glass), and the Clinical Proteomic Tumor Analysis Consortium (CPTAC, https://pdc.cancer.gov/pdc/). We extracted survival data for IDH wild-type GBM patients and categorized them into high- and low-risk groups based on corresponding median CMI. Survival analyses showed that four of the seven cohorts were significantly different between the two groups (Fig. S7). The above results indicated that the CMRGS constructed in this study could well predict the prognosis of glioma patients.

In addition, we selected modeling genes S100A11 for experimental validation using samples from patients collected during

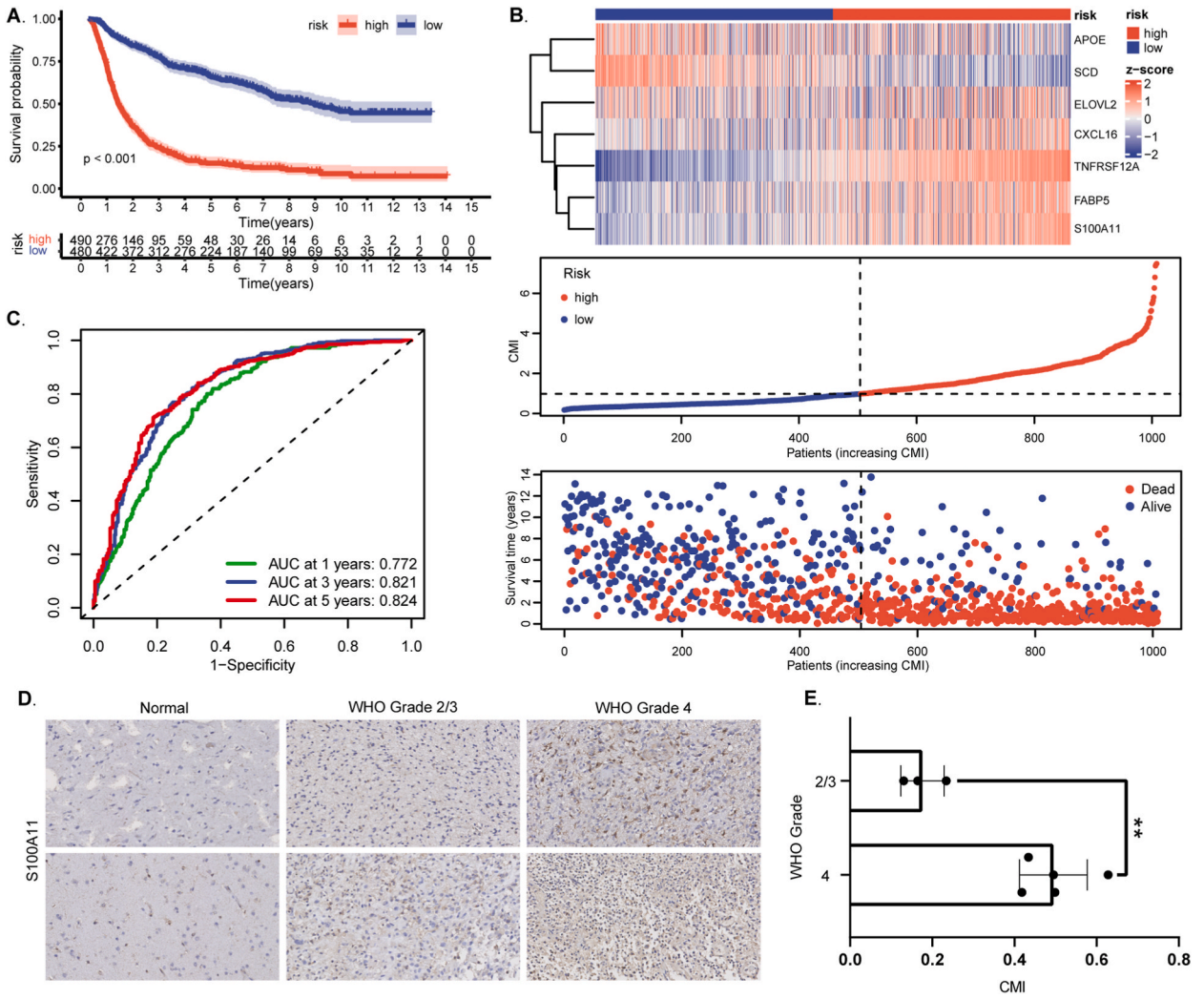

Fig. 7. Validation of CMRGS in External Cohorts. (A) Survival curve of high- and low-risk groups in TCGA cohorts. (B) Heatmap of the modeling genes expression in groups (upper), the distribution and median value of CMI (middle), and the distributions of survival status, survival time, and CMI (below). The redder, the higher the gene expression; the bluer, the lower the gene expression. (C) Time-dependent ROC analysis of CMRGS. (D) Immunohistochemical staining of S100A11 in different WHO-grade glioma tissues. (E) CMI of different WHO grade gliomas calculated based on seven genes' expression. CMRGS, Cholesterol-Metabolism-related genes signature; CGGA, Chinese Glioma Genome Atlas; CMI, cholesterol metabolism index; ROC, receiver operating characteristic.

surgeries (referred to as Gusu Cohort). The results of immunohistochemical staining showed that the expression of S100A11 was higher in glioma patients than in normal tissues, and the expression was higher in WHO grade 4 than in WHO grade 2/3 (Fig. 7D). In addition, CMI calculated based on different WHO-grade tumor tissues also showed significant differences (Fig. 7E). Together, these data suggest that CMRGS is universally applicable to the prognostic assessment of glioma patients.

3.9. Accurate selection of drugs across risk groups

To identify appropriate drugs for CMRGS-stratified patients, we utilized the oncoPredict algorithm to predict the sensitivity of different drugs in glioma patients in the TCGA and CGGA cohorts. Thirty FDA-approved drugs were identified in the GDSC2 pharmacogenomic dataset, which had different IC_{50} in the high- and low-risk groups (Fig. 8A). A total of 16 drugs were sensitive in high-risk patients and 14 drugs were sensitive in low-risk patients. Seven of the total eight chemotherapeutic agents were relatively sensitive to high-risk patients, targeting primarily DNA replication (Cisplatin, Gemcitabine, Epirubicin, Topotecan, and Teniposide), mitosis (Vinorelbine), and the cell cycle (Dactinomycin). Only cyclophosphamide was more sensitive in low-risk patients (targeting DNA replication). Meanwhile, 9 out of 22 molecularly targeted drugs were relatively sensitive to high-risk patients, mainly targeting ERK MAPK signaling (Trametinib, Dabrafenib, and Selumetinib), RTK signaling (Dasatinib and Crizotinib), and DNA replication (Irinotecan), genomic integrity (Talazoparib), PI3K/MTOR signaling (Rapamycin), and protein stability and degradation (Bortezomib). To

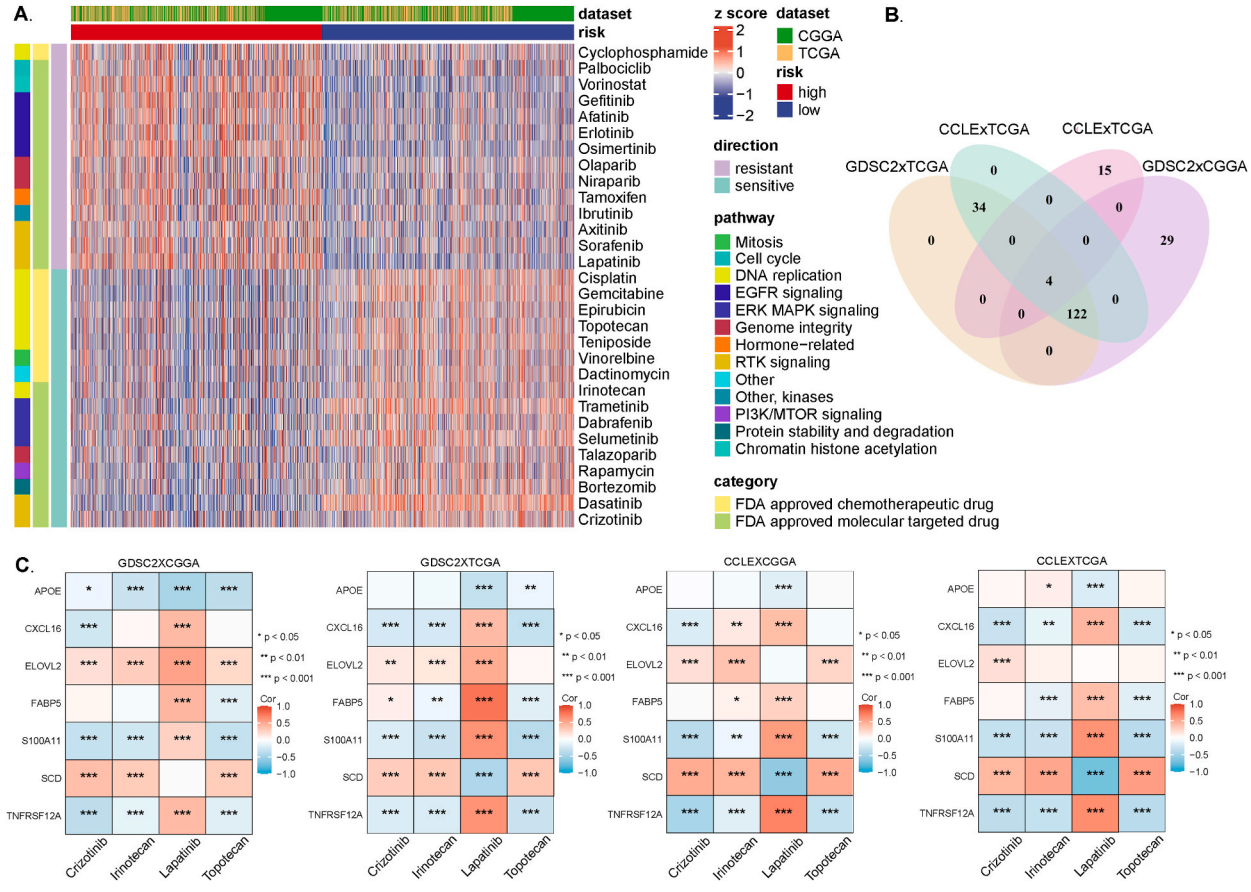

Fig. 8. Identification of chemotherapeutic and molecularly targeted drugs based on CMRGS. (A) Predicted IC_{50} of 30 FDA-approved drugs in GDSC2 in groups from TCGA and CGGA cohorts. The redder, the higher the gene expression; the bluer, the lower the gene expression. (B) Venn diagram for various combinations of training and testing sets. (C) Correlation between predicted IC_{50} of four drugs (Irinotecan, Topotecan, Crizotinib, and Lapatinib) and seven genes for CMRGS among different combinations of training and test sets. CMRGS, Cholesterol-Metabolism-related genes signature; FDA, Food and Drug Administration; IC_{50}: half-maximal inhibitory concentration; GDSC2: Drug Sensitivity in Cancer v2; TCGA, The Cancer Genome Atlas; CGGA, Chinese Glioma Genome Atlas. ***p < 0.001, **p < 0.01, *p < 0.05.

further screen potential drugs, we performed the same analysis in the CCLE pharmacogenomic dataset as in the GDSC2 dataset (Fig. 8B). Finally, Irinotecan and Topotecan (both topoisomerase inhibitors, drug target: TOP1 and TOP1MT, drug target pathway: DNA replication), Crizotinib (an ALK tyrosine kinase receptor inhibitor, drug target: ALK and MET, drug target pathway: RTK signaling) and Lapatinib (an EGFR inhibitor, drug target: EGFR and ERBB2, drug target pathway: RTK signaling) were identified in both databases. In addition, we performed Spearman correlation analysis to clarify the potential association between the predicted IC_{50} of the four screened drugs and the seven DEGs of CMRGS (Fig. 8C). The IC_{50} of Crizotinib was positively correlated with the expression of SCD and ELOVL2, the IC50 of Irinotecan and Topotecan was positively correlated with the expression of SCD, and the IC_{50} of Lapatinib was positively correlated with the expression of CXCL16, FABP5, S100A11, and TNFRSF12A. In both the US National Cancer Institute 60 anticancer drug screen (NCI-60) and Profiling Relative Inhibition Simultaneously in Mixtures (PRISM) datasets, these four drugs had low IC_{50} in CNS/brain tissues, suggesting the possibility of future application in glioma (Figs. S8 and S9).

4. Discussion

Cholesterol is an essential component of biological membranes and serves as a precursor for the synthesis of steroid hormones [36]. In recent years, a growing body of research has revealed that solid tumors exhibit distinct characteristics in cholesterol metabolism compared to normal tissue [37]. Glioblastoma is a highly aggressive tumor of the CNS that seriously affects the survival of patients [38]. Several reviews have reported the characterization of cholesterol metabolism in gliomas and the potential promise of targeting cholesterol synthesis and homeostasis, including cholesterol uptake and promotion of cholesterol efflux and disruption of cellular cholesterol transport to inhibit tumor growth [15,16,39,40]. In normal brain tissue, astrocytes are responsible for synthesizing most of the cholesterol required to maintain homeostasis in the brain [15]. However, glioblastoma cells primarily depend on exogenous cholesterol uptake rather than de novo synthesis [16]. The tumor microenvironment, composed of tumor cells, immune cells,

extracellular matrix, and various signaling molecules, plays a crucial role in glioblastoma biology [41]. Tumor-associated macrophages (TAMs) are instrumental in the glioblastoma microenvironment [42]. Fatty acids, Fatty acids, the binding partners of most cholesterol, play a pivotal role in the polarization of TAMs, glioblastoma stem cell (GSC) self-renewal, and glioblastoma invasion [43,44]. LDL typically enters the cell membrane through LDL receptors to maintain cholesterol metabolism equilibrium. These reports collectively suggest a close association between cholesterol metabolism and glioblastoma [15]. Recent research indicates that solid tumors, including glioblastoma, exhibit atypical cholesterol metabolism features, driving the interest in understanding how cholesterol metabolism influences the tumor microenvironment (TME) and exploring potential therapeutic strategies related to cholesterol metabolism. While some tumors have employed cholesterol metabolism-related genes as prognostic markers [27,28,45–47], there is an ongoing quest to identify more precise biomarkers to aid in predicting the prognosis of cancer patients, especially those with gliomas. Nevertheless, the application of these prognostic markers still faces certain limitations.

In this study, by combining difference-in-difference analysis, univariate/multivariate Cox regression, and LASSO regression analysis, we successfully identified seven cholesterol metabolism-related genes (CMRGs) significantly associated with the prognosis of patients with gliomas, which included CXCL16, FABP5, S100A11, TNFRSF12A, ELOVL2, APOE, and SCD. We further constructed a cholesterol metabolism index (CMI) using these CMRGs. Patients in the training cohort were then divided into high- and low-risk groups based on the median CMI. A series of assessments showed significant differences between groups in terms of survival analysis and immune infiltration analysis. ROC curves further indicated that CMI effectively predicted overall survival with a predictive accuracy that exceeded, to some extent, accepted classical factors such as WHO grade, histological classification, IDH mutation status, 1p19q co-deletion status, and MGMT promoter methylation. To better understand the implications of these results, we evaluated the correlation between CMRGs and glioma immune profiles. The results demonstrated notable distinctions in anti-tumor immune activation, ESTIMATE scores, immune scores, and stromal scores between high- and low-risk groups. In addition, data from the CGGA cohort and our glioma cohort further highlight the strong prognostic prediction and immune pattern of CMRGs in gliomas.

These CMRGs have been reported to be present in a wide range of tumors and are differentially expressed in normal and corresponding tumor tissues (Figs. S10 and S11). S100A11 is a protein-coding gene responsible for calcium ion binding and calcium-dependent protein binding. Previous studies have found elevated expression of S100A11 and association with adverse prognosis in various cancers such as intrahepatic cholangiocarcinoma [48,49], malignant pleural mesothelioma [50], cervical cancer [51,52], lung adenocarcinoma [53,54], thyroid papillary carcinoma [55], colon cancer [56–58], pancreatic cancer [59,60], and ovarian cancer [61,62]. Experimental evidence supports the role of S100A11 in promoting tumor cell growth, epithelial-mesenchymal transition (EMT), migration, invasion, and glioblastoma stem cell (GSC) generation [49,52]. The work of Tu et al. showed that overexpression of S100A11 promoted GBM cell growth, EMT, migration, invasion, and generation of GSCs, whereas its knockdown inhibited these activities [63]. Work by Wang et al. suggests that interfering with the expression of S100A11 significantly inhibits glioma proliferation in vitro and tumorigenicity in vivo [64]. Our data suggest that S100A11 is highly expressed in gliomas and positively correlates with pathological grading, which is consistent with previous studies.

ELOVL2 is involved in the elongation of fatty acids, biosynthesis of polyunsaturated fatty acids, and very-long-chain fatty acids in various tissues, including the liver and brain [65], and has been reported to be involved in the development of a variety of cancers, including breast cancer [66], liposarcoma [67], and glioblastoma [68]. Earlier studies have suggested that inhibiting ELOVL2 can slow glioblastoma growth through the disruption of cell membrane phospholipids and inhibition of epidermal growth factor receptor (EGFR) signaling [69]. FABP5 (Fatty Acid Binding Protein 5) encodes the epidermal-type fatty acid-binding protein [70]. FABP5 is highly expressed in glioma tissues and enhances the malignancy of gliomas by inducing IKKα transformation and activating the NF-κB pathway [71,72]. CXCL16, or C-X-C Motif Chemokine Ligand 16, functions as an extracellular chemokine [73]. It has been shown that CXCL16 release is involved in regulating the anti-inflammatory/pro-tumorigenic phenotype of glioma-associated microglia/macrophages (GAMs). CXCL16/CXCR6 signaling acts directly on mouse glioma cells as well as primary human GBM cells to promote tumor cell growth, migration, and invasion [74]. Recently, Chia et al. proposed the CXCL16-CXCR6 axis in glioblastoma modulates T-cell activity in a spatiotemporal context [75].

TNFRSF12A, also known as FN14, positively regulates the extrinsic apoptosis signaling pathway and wound healing [76,77]. TNFRSF12A is typically expressed at low levels in normal, undamaged brain tissue but is significantly upregulated in solid tumors, including glioblastoma [78]. This gene encodes the TNFSF12/TWEAK receptor, which, upon binding to its ligand, can activate pathways such as NF-κB, potentially contributing to glioblastoma cell migration, invasion, and resistance to ex vivo chemotherapy drugs [78,79]. Together with our findings, these findings highlight the strong association between high expression of these genes and poor prognosis in glioma patients, reinforcing the prognostic potential of CMRGs.

The protein encoded by the APOE is involved in lipid transport via a receptor-dependent pathway [80,81]. In a study focused on IDH-wildtype glioblastoma, IDH mutations induce upregulation of APOE, enhancing cholesterol efflux from glioblastoma cells, subsequently inducing M1-polarized glioma-associated microglia/macrophages (GAMs), and inhibiting glioblastoma cell invasion [82]. Similar to APOE, overexpression of SCD leads to lipid redistribution within glioblastoma cell organelles. Experiments suggest that silencing SCD restores organelle morphology in IDH1-mutant glioblastomas, potentially providing therapeutic benefits [83]. Together, these findings suggest that APOE and SCD may antagonize the malignant biological behavior of glioblastoma by regulating lipid distribution.

Moreover, we validated it using the CGGA cohort as well as our Gusu cohort. These results consistently demonstrate the robust and reliable prognostic predictive ability of CMRGS for a wide range of glioma patients with diverse clinical characteristics.

Drug sensitivity prediction analysis is widely used to guide cancer chemotherapy or targeted therapy [84–87]. Finally, it was evaluated whether CMRGS could help guide the selection of chemically and molecularly targeted drugs based on pharmacogenomic datasets (GDSC2 and CCLE) and tumor datasets (TCGA and CGGA). The high- and low-risk groups corresponded to different drugs with

lower IC50, respectively. Further correlations were found between the four FDA-approved drugs and the transcript levels of seven CMRGs: Crizotinib's IC50 positively correlates with the expression of SCD and ELOVL2, Irinotecan and Topotecan's IC50 positively correlates with SCD expression, and Lapatinib's IC50 positively correlates with the expression of CXCL16, FABP5, S100A11, and TNFRSF12A. These carefully selected drugs exhibited low IC50 values in the NCI-60 and PRISM datasets, highlighting their considerable potential application in glioblastoma patients. A phase Ib clinical trial has shown that adding Crizotinib to standard radiation and temozolomide treatment for newly diagnosed glioblastoma patients not only exhibited reliable safety but also yielded promising therapeutic results [88]. Another phase II clinical trial found that Bevacizumab in combination with Irinotecan treatment reduced the risk of disease progression in glioblastoma patients, although it did not significantly improve overall survival or patient's quality of life [89]. As for the role of Topotecan in glioblastoma treatment, clinical studies revealed better outcomes in terms of six-month progression-free survival and progression-free survival when compared to patients receiving radiation therapy alone [90]. In recurrent central nervous system malignant tumors in children, Lapatinib demonstrated good tolerance, although further investigations are required to determine the required drug concentration for intra-tumoral efficacy [91]. These evidences suggest that CMRGS-assisted drug screening is expected to guide individualized treatment and deserves to be further investigated in depth.

Our work systematically explored the role of cholesterol metabolism-related genes in prognosis prediction and selection of personalized treatment regimens for glioma patients. However, this study has certain limitations. Firstly, our current results primarily stem from the TCGA and CGGA databases. TCGA mainly collects samples from European and American populations, while CGGA focuses on Chinese patients. Such geographical and ethnic differences may lead to limited applicability of the data globally. In addition, different sequencing platforms and experimental procedures may lead to systematic bias and affect the comparability of data. Of particular importance, Bulk RNA-seq measures the average expression level of all cells in a sample and is unable to distinguish between the specific expression of different cell types, which may result in the masking of critical biological information. Bulk RNA-seq data similarly fail to provide information on the spatial distribution of cells in a tissue, limiting the understanding of the tumor microenvironment. Given the critical role of cholesterol metabolism in the malignant phenotype of tumor cells, further studies should explore its role at multiple levels: genomic, transcriptomic, proteomic, modifier, and metabolomic.

CRediT authorship contribution statement

Dengfeng Lu: Software, Methodology, Conceptualization. **Fei Wang:** Methodology. **Yayi Yang:** Writing – original draft, Visualization. **Aojie Duan:** Visualization. **Yubo Ren:** Data curation. **Yun Feng:** Software, Formal analysis. **Haiying Teng:** Validation, Data curation. **Zhouqing Chen:** Writing – review & editing, Supervision, Funding acquisition. **Xiaoou Sun:** Writing – review & editing, Funding acquisition. **Zhong Wang:** Project administration.

Funding

This work was supported by Soochow University Horizontal Projects (H231052, H230786, and H240117 for Xiaoou Sun) and the National Natural Science Foundation of China (No. 82201445 for Zhouqing Chen).

Declaration of competing interest

The authors declare that they have no known competing financial interests or personal relationships that could have appeared to influence the work reported in this paper.

Acknowledgments

None.

Appendix A. Supplementary data

Supplementary data to this article can be found online at https://doi.org/10.1016/j.heliyon.2024.e41601.

References

[1] S. Xu, L. Tang, X. Li, F. Fan, Z. Liu, Immunotherapy for glioma: current management and future application, Cancer Lett. 476 (2020).
[2] K. Yang, Z. Wu, H. Zhang, N. Zhang, W. Wu, Z. Wang, Z. Dai, X. Zhang, L. Zhang, Y. Peng, W. Ye, W. Zeng, Z. Liu, Q. Cheng, Glioma targeted therapy: insight into future of molecular approaches, Mol. Cancer 21 (1) (2022) 39.
[3] M. Weller, E. Le Rhun, How did lomustine become standard of care in recurrent glioblastoma? Cancer Treat Rev. 87 (2020) 102029.
[4] D. Sonkin, A. Thomas, B.A. Teicher, Cancer treatments: past, present, and future, Cancer Genet 286–287 (2024) 18–24.
[5] M. Cheng, Z.W. Zhang, X.H. Ji, Y. Xu, E. Bian, B. Zhao, Super-enhancers: a new frontier for glioma treatment, Biochim. Biophys. Acta Rev. Canc 1873 (2) (2020) 188353.
[6] H. Wang, T. Xu, Q. Huang, W. Jin, J. Chen, Immunotherapy for malignant glioma: current status and future directions, Trends Pharmacol. Sci. 41 (2) (2020) 123–138.

[7] E. Sezgin, I. Levental, S. Mayor, C. Eggeling, The mystery of membrane organization: composition, regulation and roles of lipid rafts, Nat. Rev. Mol. Cell Biol. 18 (6) (2017) 361–374.
[8] D.S. Schade, L. Shey, R.P. Eaton, Cholesterol review: a metabolically important molecule, Endocr. Pract. 26 (12) (2020) 1514–1523.
[9] R.Y. Hampton, A cholesterol toggle switch, Cell Metab 8 (6) (2008) 451–453.
[10] J.D. Horton, N.A. Shah, J.A. Warrington, N.N. Anderson, S.W. Park, M.S. Brown, J.L. Goldstein, Combined analysis of oligonucleotide microarray data from transgenic and knockout mice identifies direct SREBP target genes, Proc Natl Acad Sci U S A 100 (21) (2003) 12027–12032.
[11] J.L. Goldstein, R.A. DeBose-Boyd, M.S. Brown, Protein sensors for membrane sterols, Cell 124 (1) (2006) 35–46.
[12] N. Zelcer, C. Hong, R. Boyadjian, P. Tontonoz, LXR regulates cholesterol uptake through Idol-dependent ubiquitination of the LDL receptor, Science 325 (5936) (2009) 100–104.
[13] F. Bovenga, C. Sabbà, A. Moschetta, Uncoupling nuclear receptor LXR and cholesterol metabolism in cancer, Cell Metab 21 (4) (2015) 517–526.
[14] D. Lütjohann, O. Breuer, G. Ahlborg, I. Nennesmo, A. Sidén, U. Diczfalusy, I. Björkhem, Cholesterol homeostasis in human brain: evidence for an age-dependent flux of 24S-hydroxycholesterol from the brain into the circulation, Proc Natl Acad Sci U S A 93 (18) (1996) 9799–9804.
[15] F. Ahmad, Q. Sun, D. Patel, J.M. Stommel, Cholesterol metabolism: a potential therapeutic target in glioblastoma, Cancers 11 (2) (2019).
[16] X. Guo, S. Zhou, Z. Yang, Z.-A. Li, W. Hu, L. Dai, W. Liang, X. Wang, Cholesterol metabolism and its implication in glioblastoma therapy, J. Cancer 13 (6) (2022) 1745–1757.
[17] Y. Yoshioka, J. Sasaki, M. Yamamoto, K. Saitoh, S. Nakaya, M. Kubokawa, Quantitation by (1)H-NMR of dolichol, cholesterol and choline-containing lipids in extracts of normal and phathological thyroid tissue, NMR Biomed. 13 (7) (2000) 377–383.
[18] Y. Meng, Q. Wang, Z. Lyu, Cholesterol metabolism and tumor, Zhejiang Da Xue Xue Bao Yi Xue Ban 50 (1) (2021) 23–31.
[19] D. Guo, F. Reinitz, M. Youssef, C. Hong, D. Nathanson, D. Akhavan, D. Kuga, A.N. Amzajerdi, H. Soto, S. Zhu, I. Babic, K. Tanaka, J. Dang, A. Iwanami, B. Gini, J. Dejesus, D.D. Lisiero, T.T. Huang, R.M. Prins, P.Y. Wen, H.I. Robins, M.D. Prados, L.M. Deangelis, I.K. Mellinghoff, M.P. Mehta, C.D. James, A. Chakravarti, T. F. Cloughesy, P. Tontonoz, P.S. Mischel, An LXR agonist promotes glioblastoma cell death through inhibition of an EGFR/AKT/SREBP-1/LDLR-dependent pathway, Cancer Discov. 1 (5) (2011) 442–456.
[20] Z. Qiu, W. Yuan, T. Chen, C. Zhou, C. Liu, Y. Huang, D. Han, Q. Huang, HMGCR positively regulated the growth and migration of glioblastoma cells, Gene 576 (1 Pt 1) (2016) 22–27.
[21] L. Zhao, Z. Qiu, Z. Yang, L. Xu, T.M. Pearce, Q. Wu, K. Yang, F. Li, O. Saulnier, F. Fei, H. Yu, R.C. Gimple, V. Varadharajan, J. Liu, L.D. Hendrikse, V. Fong, W. Wang, J. Zhang, D. Lv, D. Lee, B.M. Lehrich, C. Jin, L. Ouyang, D. Dixit, H. Wu, X. Wang, A.E. Sloan, X. Wang, T. Huan, J. Mark Brown, S.A. Goldman, M. D. Taylor, S. Zhou, J.N. Rich, Lymphatic endothelial-like cells promote glioblastoma stem cell growth through cytokine-driven cholesterol metabolism, Nat Cancer 5 (1) (2024) 147–166.
[22] G.R. Villa, J.J. Hulce, C. Zanca, J. Bi, S. Ikegami, G.L. Cahill, Y. Gu, K.M. Lum, K. Masui, H. Yang, X. Rong, C. Hong, K.M. Turner, F. Liu, G.C. Hon, D. Jenkins, M. Martini, A.M. Armando, O. Quehenberger, T.F. Cloughesy, F.B. Furnari, W.K. Cavenee, P. Tontonoz, T.C. Gahman, A.K. Shiau, B.F. Cravatt, P.S. Mischel, An LXR-cholesterol Axis creates a metabolic Co-dependency for brain cancers, Cancer Cell 30 (5) (2016) 683–693.
[23] Y. Dong, J. Zhang, Y. Wang, Y. Zhang, D. Rappaport, Z. Yang, M. Han, Y. Liu, Z. Fu, X. Zhao, C. Tang, C. Shi, D. Zhang, D. Li, S. Ni, A. Li, J. Cui, T. Li, P. Sun, O. Benny, C. Zhang, K. Zhao, C. Chen, X. Jiang, Intracavitary spraying of nanoregulator-encased hydrogel modulates cholesterol metabolism of glioma-supportive macrophage for postoperative glioblastoma immunotherapy, Adv Mater 36 (13) (2024) e2311109.
[24] N. Yin, Y. Wang, Y. Liu, R. Niu, S. Zhang, Y. Cao, Z. Lv, S. Song, X. Liu, H. Zhang, A cholesterol metabolic regulated hydrogen-bonded organic framework (HOF)-Based biotuner for antibody non-dependent immunotherapy tailored for glioblastoma, Adv Mater 35 (44) (2023) e2303567.
[25] H. Liu, R. Xie, Q. Dai, J. Fang, Y. Xu, B. Li, Exploring the mechanism underlying hyperuricemia using comprehensive research on multi-omics, Sci. Rep. 13 (1) (2023) 7161.
[26] K.H. Stopsack, T.A. Gerke, J.A. Sinnott, K.L. Penney, S. Tyekucheva, H.D. Sesso, S.-O. Andersson, O. Andrén, J.R. Cerhan, E.L. Giovannucci, L.A. Mucci, J. R. Rider, Cholesterol metabolism and prostate cancer lethality, Cancer Res. 76 (16) (2016) 4785–4790.
[27] W. Tang, G. Li, Q. Lin, Z. Zhu, Z. Wang, Z. Wang, Multiplex immunohistochemistry defines two cholesterol metabolism patterns predicting immunotherapeutic outcomes in gastric cancer, J. Transl. Med. 21 (1) (2023) 887.
[28] S. Kuldeep, S. Soni, A. Srivastava, A. Mishra, L.K. Sharma, C.C. Mandal, Dysregulated cholesterol regulatory genes as a diagnostic biomarker for cancer, J. Gene Med. 25 (4) (2023) e3475.
[29] H. Liu, T. Tang, MAPK signaling pathway-based glioma subtypes, machine-learning risk model, and key hub proteins identification, Sci. Rep. 13 (1) (2023) 19055.
[30] D. Lu, Y. Wang, G. Liu, S. Wang, A. Duan, Z. Wang, J. Wang, X. Sun, Y. Wu, Z. Wang, Armcx1 attenuates secondary brain injury in an experimental traumatic brain injury model in male mice by alleviating mitochondrial dysfunction and neuronal cell death, Neurobiol. Dis. 184 (2023) 106228.
[31] Y. Yang, F. Wang, H. Teng, C. Zhang, Y. Zhang, P. Chen, Q. Li, X. Kan, Z. Chen, Z. Wang, Y. Yu, Integrative analysis of multi-omics data reveals a pseudouridine-related lncRNA signature for prediction of glioma prognosis and chemoradiotherapy sensitivity, Comput. Biol. Med. 166 (2023) 107428.
[32] N. Feizi, S.K. Nair, P. Smirnov, G. Beri, C. Eeles, P.N. Esfahani, M. Nakano, D. Tkachuk, A. Mammoliti, E. Gorobets, A.S. Mer, E. Lin, Y. Yu, S. Martin, M. Hafner, B. Haibe-Kains, PharmacoDB 2.0: improving scalability and transparency of in vitro pharmacogenomics analysis, Nucleic Acids Res. 50 (D1) (2022) D1348–D1357.
[33] L. Tang, R. Wei, R. Chen, G. Fan, J. Zhou, Z. Qi, K. Wang, Q. Wei, X. Wei, X. Xu, Establishment and validation of a cholesterol metabolism-related prognostic signature for hepatocellular carcinoma, Comput. Struct. Biotechnol. J. 20 (2022) 4402–4414.
[34] A. Liberzon, A. Subramanian, R. Pinchback, H. Thorvaldsdóttir, P. Tamayo, J.P. Mesirov, Molecular signatures database (MSigDB) 3.0, Bioinformatics 27 (12) (2011) 1739–1740.
[35] A. Subramanian, P. Tamayo, V.K. Mootha, S. Mukherjee, B.L. Ebert, M.A. Gillette, A. Paulovich, S.L. Pomeroy, T.R. Golub, E.S. Lander, J.P. Mesirov, Gene set enrichment analysis: a knowledge-based approach for interpreting genome-wide expression profiles, Proceedings of the National Academy of Sciences of the United States of America 102 (43) (2005) 15545–15550.
[36] M. Gliozzi, V. Musolino, F. Bosco, M. Scicchitano, F. Scarano, S. Nucera, M.C. Zito, S. Ruga, C. Carresi, R. Macrì, L. Guarnieri, J. Maiuolo, A. Tavernese, A. R. Coppoletta, C. Nicita, R. Mollace, E. Palma, C. Muscoli, C. Belzung, V. Mollace, Cholesterol homeostasis: researching a dialogue between the brain and peripheral tissues, Pharmacol. Res. 163 (2021) 105215.
[37] M. Xiao, J. Xu, W. Wang, B. Zhang, J. Liu, J. Li, H. Xu, Y. Zhao, X. Yu, S. Shi, Functional significance of cholesterol metabolism in cancer: from threat to treatment, Exp. Mol. Med. 55 (9) (2023) 1982–1995.
[38] M. Weller, P.Y. Wen, S.M. Chang, L. Dirven, M. Lim, M. Monje, G. Reifenberger, Glioma. Nat Rev Dis Primers 10 (1) (2024) 33.
[39] Y. Kou, F. Geng, D. Guo, Lipid metabolism in glioblastoma: from de novo synthesis to storage, Biomedicines 10 (8) (2022).
[40] L. Pirmoradi, N. Seyfizadeh, S. Ghavami, A.A. Zeki, S. Shojaei, Targeting cholesterol metabolism in glioblastoma: a new therapeutic approach in cancer therapy, J Investig Med 67 (4) (2019) 715–719.
[41] H. Lin, C. Liu, A. Hu, D. Zhang, H. Yang, Y. Mao, Understanding the immunosuppressive microenvironment of glioma: mechanistic insights and clinical perspectives, J. Hematol. Oncol. 17 (1) (2024) 31.
[42] F. Khan, L. Pang, M. Dunterman, M.S. Lesniak, A.B. Heimberger, P. Chen, Macrophages and microglia in glioblastoma: heterogeneity, plasticity, and therapy, J. Clin. Invest. 133 (1) (2023).
[43] Y. Teng, L. Xu, W. Li, P. Liu, L. Tian, M. Liu, Targeting reactive oxygen species and fat acid oxidation for the modulation of tumor-associated macrophages: a narrative review, Front. Immunol. 14 (2023) 1224443.
[44] J. Miska, N.S. Chandel, Targeting fatty acid metabolism in glioblastoma, J. Clin. Invest. 133 (1) (2023).
[45] S. Li, Z. Zheng, B. Wang, Machine learning survival prediction using tumor lipid metabolism genes for osteosarcoma, Sci. Rep. 14 (1) (2024) 12934.
[46] H. Lei, T. Xiang, H. Zhu, X. Hu, A novel cholesterol metabolism-related lncRNA signature predicts the prognosis of patients with hepatocellular carcinoma and their response to immunotherapy, Front Biosci (Landmark Ed) 29 (3) (2024) 129.

[47] Y. He, X. Cui, Y. Lin, Y. Wang, D. Wu, Y. Fang, Using elevated cholesterol synthesis as a prognostic marker in wilms' tumor: a bioinformatic analysis, BioMed Res. Int. 2021 (2021) 8826286.

[48] M.-X. Zhang, W. Gan, C.-Y. Jing, S.-S. Zheng, Y. Yi, J. Zhang, X. Xu, J.-J. Lin, B.-H. Zhang, S.-J. Qiu, S100A11 promotes cell proliferation via P38/MAPK signaling pathway in intrahepatic cholangiocarcinoma, Mol. Carcinog. 58 (1) (2019) 19–30.

[49] M. Zhang, S. Zheng, C. Jing, J. Zhang, H. Shen, X. Xu, J. Lin, B. Zhang, S100A11 promotes TGF-β1-induced epithelial-mesenchymal transition through SMAD2/3 signaling pathway in intrahepatic cholangiocarcinoma, Future Oncol. 14 (9) (2018) 837–847.

[50] H. Sato, M. Sakaguchi, H. Yamamoto, S. Tomida, K. Aoe, K. Shien, T. Yoshioka, K. Namba, H. Torigoe, J. Soh, K. Tsukuda, H. Tao, K. Okabe, S. Miyoshi, H. I. Pass, S. Toyooka, Therapeutic potential of targeting S100A11 in malignant pleural mesothelioma, Oncogenesis 7 (1) (2018) 11.

[51] M. Maděrka, V. Dvořák, J. Hambálek, D. Stejskal, Krejčí, M. Švesták, K. Langová, R. Pilka, Serum concentrations of S100-A11 and AIF-1 are elevated in cervical cancer patients with lymph node involvement, Ceska Gynekol. 86 (1) (2021) 17–21.

[52] M. Meng, L. Sang, X. Wang, S100 calcium binding protein A11 (S100A11) promotes the proliferation, migration and invasion of cervical cancer cells, and activates wnt/β-catenin signaling, OncoTargets Ther. 12 (2019) 8675–8685.

[53] T. Woo, K. Okudela, H. Mitsui, M. Tajiri, Y. Rino, K. Ohashi, M. Masuda, Up-regulation of S100A11 in lung adenocarcinoma - its potential relationship with cancer progression, PLoS One 10 (11) (2015) e0142642.

[54] J. Hao, K. Wang, Y. Yue, T. Tian, A. Xu, J. Hao, X. Xiao, D. He, Selective expression of S100A11 in lung cancer and its role in regulating proliferation of adenocarcinomas cells, Mol. Cell. Biochem. 359 (1–2) (2012) 323–332.

[55] M.C. Anania, C. Miranda, M.G. Vizioli, M. Mazzoni, L. Cleris, S. Pagliardini, G. Manenti, M.G. Borrello, M.A. Pierotti, A. Greco, S100A11 overexpression contributes to the malignant phenotype of papillary thyroid carcinoma, J. Clin. Endocrinol. Metab. 98 (10) (2013) E1591–E1600.

[56] W. Li, F. Han, K. Tang, C. Ding, F. Xiong, Y. Xiao, C. Li, Q. Liang, K.Y. Lee, I.-S. Lee, H. Gao, Inhibiting NF-κB-S100A11 signaling and targeting S100A11 for anticancer effects of demethylzeylasteral in human colon cancer, Biomedicine & Pharmacotherapy = Biomedecine & Pharmacotherapie 168 (2023) 115725.

[57] S. Meding, B. Balluff, M. Elsner, C. Schöne, S. Rauser, U. Nitsche, M. Maak, A. Schäfer, S.M. Hauck, M. Ueffing, R. Langer, H. Höfler, H. Friess, R. Rosenberg, A. Walch, Tissue-based proteomics reveals FXYD3, S100A11 and GSTM3 as novel markers for regional lymph node metastasis in colon cancer, J. Pathol. 228 (4) (2012) 459–470.

[58] C. Melle, G. Ernst, B. Schimmel, A. Bleul, H. Mothes, R. Kaufmann, U. Settmacher, F. Von Eggeling, Different expression of calgizzarin (S100A11) in normal colonic epithelium, adenoma and colorectal carcinoma, Int. J. Oncol. 28 (1) (2006) 195–200.

[59] X. Zeng, H. Guo, Z. Liu, Z. Qin, Y. Cong, N. Ren, Y. Zhang, N. Zhang, S100A11 activates the pentose phosphate pathway to induce malignant biological behaviour of pancreatic ductal adenocarcinoma, Cell Death Dis. 13 (6) (2022) 568.

[60] Y. Mitsui, N. Tomonobu, M. Watanabe, R. Kinoshita, I.W. Sumardika, C. Youyi, H. Murata, K.-I. Yamamoto, T. Sadahira, A.G.H. Rodrigo, H. Takamatsu, K. Araki, A. Yamauchi, M. Yamamura, H. Fujiwara, Y. Inoue, J. Futami, K. Saito, H. Iioka, E. Kondo, M. Nishibori, S. Toyooka, Y. Yamamoto, Y. Nasu, M. Sakaguchi, Upregulation of mobility in pancreatic cancer cells by secreted S100A11 through activation of surrounding fibroblasts, Oncol. Res. 27 (8) (2019) 945–956.

[61] W. Li, Z. Cui, Y. Kong, X. Liu, X. Wang, Serum levels of S100A11 and MMP-9 in patients with epithelial ovarian cancer and their clinical significance, BioMed Res. Int. 2021 (2021) 7341247.

[62] Y. Li, J. Zhang, Expression of S100A11 is a prognostic factor for disease-free survival and overall survival in patients with high-grade serous ovarian cancer, Appl. Immunohistochem. Mol. Morphol. 25 (2) (2017) 110–116.

[63] Y. Tu, P. Xie, X. Du, L. Fan, Z. Bao, G. Sun, P. Zhao, H. Chao, C. Li, A. Zeng, M. Pan, J. Ji, S100A11 functions as novel oncogene in glioblastoma via S100A11/ANXA2/NF-κB positive feedback loop, J. Cell Mol. Med. 23 (10) (2019) 6907–6918.

[64] H. Wang, M. Yin, L. Ye, P. Gao, X. Mao, X. Tian, Z. Xu, X. Dai, H. Cheng, S100A11 promotes glioma cell proliferation and predicts grade-correlated unfavorable prognosis, Technol. Cancer Res. Treat. 20 (2021) 15330338211011961.

[65] A. Gómez Rodríguez, E. Talamonti, A. Naudi, A.V. Kalinovich, A.M. Pauter, G. Barja, T. Bengtsson, A. Jacobsson, R. Pamplona, I.G. Shabalina, Elovl2-Ablation leads to mitochondrial membrane fatty acid remodeling and reduced efficiency in mouse liver mitochondria, Nutrients 14 (3) (2022).

[66] H.W. Kim, M. Baek, S. Jung, S. Jang, H. Lee, S.-H. Yang, B.S. Kwak, S.J. Kim, ELOVL2-AS1 suppresses tamoxifen resistance by sponging miR-1233-3p in breast cancer, Epigenetics 18 (1) (2023) 2276384.

[67] Z. Wang, P. Tao, P. Fan, J. Wang, T. Rong, Y. Hou, Y. Zhou, W. Lu, L. Hong, L. Ma, Y. Zhang, H. Tong, Insight of a lipid metabolism prognostic model to identify immune landscape and potential target for retroperitoneal liposarcoma, Front. Immunol. 14 (2023) 1209396.

[68] J. Korbecki, D. Simińska, D. Jeżewski, K. Kojder, P. Tomasiak, M. Tarnowski, D. Chlubek, I. Baranowska-Bosiacka, Glioblastoma multiforme tumors in women have a lower expression of fatty acid elongases ELOVL2, ELOVL5, ELOVL6, and ELOVL7 than in men, Brain Sci. 12 (10) (2022).

[69] R.C. Gimple, R.L. Kidwell, L.J.Y. Kim, T. Sun, A.D. Gromovsky, Q. Wu, M. Wolf, D. Lv, S. Bhargava, L. Jiang, B.C. Prager, X. Wang, Q. Ye, Z. Zhu, G. Zhang, Z. Dong, L. Zhao, D. Lee, J. Bi, A.E. Sloan, P.S. Mischel, J.M. Brown, H. Cang, T. Huan, S.C. Mack, Q. Xie, J.N. Rich, Glioma stem cell-specific superenhancer promotes polyunsaturated fatty-acid synthesis to support EGFR signaling, Cancer Discov. 9 (9) (2019) 1248–1267.

[70] W. George Warren, M. Osborn, A. Yates, K. Wright, S.E. O'Sullivan, The emerging role of fatty acid binding protein 5 (FABP5) in cancers, Drug Discov. Today 28 (7) (2023) 103628.

[71] Y. Wang, A. Wahafu, W. Wu, J. Xiang, L. Huo, X. Ma, N. Wang, H. Liu, X. Bai, D. Xu, W. Xie, M. Wang, J. Wang, FABP5 enhances malignancies of lower-grade gliomas via canonical activation of NF-κB signaling, J. Cell Mol. Med. 25 (9) (2021) 4487–4500.

[72] Q. Tang, X. Mao, Z. Chen, C. Ma, Y. Tu, Q. Zhu, J. Lu, Z. Wang, Q. Zhang, W. Wu, Liquid-liquid phase separation-related gene in gliomas: FABP5 is a potential prognostic marker, J. Gene Med. 25 (10) (2023) e3517.

[73] J. Korbecki, K. Bajdak-Rusinek, P. Kupnicka, P. Kapczuk, D. Simińska, D. Chlubek, I. Baranowska-Bosiacka, The role of CXCL16 in the pathogenesis of cancer and other diseases, Int. J. Mol. Sci. 22 (7) (2021).

[74] F. Lepore, G. D'Alessandro, F. Antonangeli, A. Santoro, V. Esposito, C. Limatola, F. Trettel, CXCL16/CXCR6 Axis drives microglia/macrophages phenotype in physiological conditions and plays a crucial role in glioma, Front. Immunol. 9 (2018) 2750.

[75] T.-Y. Chia, L.K. Billingham, L. Boland, J.L. Katz, V.A. Arrieta, J. Shireman, A.-L. Rosas, S.L. DeLay, K. Zillinger, Y. Geng, J. Kruger, C. Silvers, H. Wang, G. I. Vazquez Cervantes, D. Hou, S. Wang, H. Wan, A. Sonabend, P. Zhang, C. Lee-Chang, J. Miska, The CXCL16-CXCR6 axis in glioblastoma modulates T-cell activity in a spatiotemporal context, Front. Immunol. 14 (2023) 1331287.

[76] J.A. Winkles, N.L. Tran, M.E. Berens, TWEAK and Fn14: new molecular targets for cancer therapy? Cancer Lett. 235 (1) (2006) 11–17.

[77] G. Hu, W. Zeng, Y. Xia, TWEAK/Fn14 signaling in tumors, Tumour Biol 39 (6) (2017) 1010428317714624.

[78] S. Yang, X. Wang, R. Huan, M. Deng, Z. Kong, Y. Xiong, T. Luo, Z. Jin, J. Liu, L. Chu, G. Han, J. Zhang, Y. Tan, Machine learning unveils immune-related signature in multicenter glioma studies, iScience 27 (4) (2024) 109317.

[79] N.P. Connolly, R. Galisteo, S. Xu, E.E. Bar, S. Peng, N.L. Tran, H.M. Ames, A.J. Kim, G.F. Woodworth, J.A. Winkles, Elevated fibroblast growth factor-inducible 14 expression transforms proneural-like gliomas into more aggressive and lethal brain cancer, Glia 69 (9) (2021) 2199–2214.

[80] A.M. Fagan, G. Bu, Y. Sun, A. Daugherty, D.M. Holtzman, Apolipoprotein E-containing high density lipoprotein promotes neurite outgrowth and is a ligand for the low density lipoprotein receptor-related protein, J. Biol. Chem. 271 (47) (1996) 30121–30125.

[81] Y. Huang, R.W. Mahley, E. Apolipoprotein, Structure and function in lipid metabolism, neurobiology, and Alzheimer's diseases, Neurobiol. Dis. 72 (2014). Pt A.

[82] T. Wang, Y. Zhou, Y. Fan, H. Duan, X. Guo, J. Chang, Y. Jiang, C. Li, Z. Fu, Y. Gao, X. Guo, K. Sidlauskas, Z. He, C. Da Costa, X. Sheng, D. Wu, J. Yuan, H. Li, Y. He, Y. Mou, N. Li, PERK-mediated cholesterol excretion from IDH mutant glioma determines anti-tumoral polarization of microglia, Adv. Sci. 10 (20) (2023) e2205949.

[83] A. Lita, A. Pliss, A. Kuzmin, T. Yamasaki, L. Zhang, T. Dowdy, C. Burks, N. de Val, O. Celiku, V. Ruiz-Rodado, E.-R. Nicoli, M. Kruhlak, T. Andresson, S. Das, C. Yang, R. Schmitt, C. Herold-Mende, M.R. Gilbert, P.N. Prasad, M. Larion, IDH1 mutations induce organelle defects via dysregulated phospholipids, Nat. Commun. 12 (1) (2021) 614.

[84] L. Ou, H. Liu, C. Peng, Y. Zou, J. Jia, H. Li, Z. Feng, G. Zhang, M. Yao, Helicobacter pylori infection facilitates cell migration and potentially impact clinical outcomes in gastric cancer, Heliyon 10 (17) (2024) e37046.

[85] H. Liu, T. Tang, Pan-cancer genetic analysis of disulfidptosis-related gene set, Cancer Genet (2023) 278–279.
[86] H. Liu, T. Tang, Pan-cancer genetic analysis of cuproptosis and copper metabolism-related gene set, Front. Oncol. 12 (2022) 952290.
[87] H. Liu, T. Tang, A bioinformatic study of IGFBPs in glioma regarding their diagnostic, prognostic, and therapeutic prediction value, Am J Transl Res 15 (3) (2023) 2140–2155.
[88] M. Martínez-García, G. Velasco, E. Pineda, M. Gil-Gil, F. Alameda, J. Capellades, M.C. Martín-Soberón, I. López-Valero, E. Tovar Ambel, P. Foro, Á. Taus, M. Arumi, A. Hernández-Laín, J.M. Sepúlveda-Sánchez, Safety and efficacy of Crizotinib in combination with temozolomide and radiotherapy in patients with newly diagnosed glioblastoma: phase Ib GEINO 1402 trial, Cancers 14 (10) (2022).
[89] U. Herrlinger, N. Schäfer, J.P. Steinbach, A. Weyerbrock, P. Hau, R. Goldbrunner, F. Friedrich, V. Rohde, F. Ringel, U. Schlegel, M. Sabel, M.W. Ronellenfitsch, M. Uhl, J. Maciaczyk, S. Grau, O. Schnell, M. Hänel, D. Krex, P. Vajkoczy, R. Gerlach, R.-D. Kortmann, M. Mehdorn, J. Tüttenberg, R. Mayer-Steinacker, R. Fietkau, S. Brehmer, F. Mack, M. Stuplich, S. Kebir, R. Kohnen, E. Dunkl, B. Leutgeb, M. Proescholdt, T. Pietsch, H. Urbach, C. Belka, W. Stummer, M. Glas, Bevacizumab plus irinotecan versus temozolomide in newly diagnosed O6-methylguanine-DNA methyltransferase nonmethylated glioblastoma: the randomized GLARIUS trial, J. Clin. Oncol. 34 (14) (2016) 1611–1619.
[90] G.G. Grabenbauer, K.-D. Gerber, O. Ganslandt, A. Richter, G. Klautke, J. Birkmann, M. Meyer, Effects of concurrent topotecan and radiation on 6-month progression-free survival in the primary treatment of glioblastoma multiforme, Int. J. Radiat. Oncol. Biol. Phys. 75 (1) (2009) 164–169.
[91] M. Fouladi, C.F. Stewart, S.M. Blaney, A. Onar-Thomas, P. Schaiquevich, R.J. Packer, S. Goldman, J.R. Geyer, A. Gajjar, L.E. Kun, J.M. Boyett, R.J. Gilbertson, A molecular biology and phase II trial of lapatinib in children with refractory CNS malignancies: a pediatric brain tumor consortium study, J. Neuro Oncol. 114 (2) (2013) 173–179.